DETECTING THE DURATION OF INCOMPLETE OBSTRUCTIVE SLEEP APNEA EVENTS USING INTERHEMISPHERIC FEATURES OF ELECTROENCEPHALOGRAPHY

CHIEN-CHANG HSU[1], ZHEN-GJIA CAI[1], HSING MEI[1]
HOU-CHANG CHIU[2,3] AND CHIA-MO LIN[2,4]

[1]Department of Computer Science and Information Engineering
[2]School of Medicine
Fu Jen Catholic University
No. 510, Chung Cheng Rd., Hsinchuang Dist., New Taipei City 242, Taiwan
{ cch; mei }@csie.fju.edu.tw; a124136906@yahoo.com.tw

[3]Department of Neurology
[4]Sleep Center
Shin Kong Wu Ho-Su Memorial Hospital
No. 95, Wen Chang Rd., Shih Lin Dist., Taipei City 111, Taiwan
{ 054885; 081810 }@mail.fju.edu.tw

ABSTRACT. *Obstructive sleep apnea not only affects sleep quality, it can also be life-threatening. For diagnosis and treatment, most clinicians use a patient's sleep data recorded by polysomnography. However, the amount of overnight sleep data is massive, which makes efficient and comprehensive data interpreting extremely challenging. Numerous detection methods have been developed; however, the accuracy of these methods must be improved. This work transforms electroencephalogram signals from the left and right hemispheres using a novel obstructive sleep apnea (OSA) detection system, and extracts signal features of delta waves using a bandpass filter, empirical mode decomposition, and Hilbert-Huang transformation. The start or end time of an incomplete OSA event is predicted based on the relationship between the time and frequency variation of detected complete OSA events. Experimental results demonstrate that the proposed system is accurate in detecting the frequency and duration of incomplete OSA events, and system performance is better than that of existing detection methods. The proposed system will provide useful auxiliary diagnostic data for physicians and technicians at sleep centers.*
Keywords: Obstructive sleep apnea, Electroencephalogram, Frequency variation, Incomplete obstructive sleep apnea event, Start or end time prediction

1. **Introduction.** Obstructive sleep apnea (OSA) is a syndrome characterized by interruption of airflow for 10 s to 2 min or obstruction of the upper respiratory tract. Once the brain senses that the oxygen supply is insufficient, the brain is aroused and instructs the body to move around or wake up to resume breathing. Notably, OSA affects the sleep quality of countless people. People with OSA are often unaware that they have OSA, even though their breathing is interrupted numerous times while sleeping, adversely affecting their sleep, resulting in lethargy during waking hours and poor concentration [2,11,21,35]. Over the long term, OSA affects cardiopulmonary functions and may cause sudden unexpected nocturnal death syndrome [1]. Symptoms of OSA have garnered much attention from the medical community in recent years. Common indicators for sleep disorders include the apnea index (AI), respiratory disturbance index (RDI), and apnea and hypopnea index (AHI) [2,30].

Human brainwaves, which generate spontaneous and event-related electroencephalogram (EEG) signals, facilitate observations of various sleep signals [3,13,19,20,25,27,34]. Brainwave features are utilized when diagnosing various sleep disorders. Basically, the major spectrums of a sleep EEG are delta (0-4 Hz), theta (4-8 Hz), alpha (8-16 Hz), and beta (16-32 Hz) signals. Delta and theta signals provide useful data for identifying OSA events [30]. Currently, common methods for OSA event detection using EEG signals include statistical, time-frequency, and frequency variation approaches [2,22,23,29,30]. The statistical approach uses statistical characteristics, such as mean and standard deviation, to identify correlations among various spectrum features. However, features of brainwaves are extremely complex, and identifying effective transient variations in the brain is difficult. Additionally, identifying pathological correlations using a large number of statistical computations is a very complex process [10]. Therefore, precisely detecting the duration of an OSA event is a significant challenge. The time-frequency approach uses non-linear signal features to quantify time-frequency relationships such as approximate entropy and complexity calculations. The disadvantage of the time-frequency approach is that only a portion of each band of brainwave can be observed. Additionally, this approach cannot manage transient variations in brainwaves during OSA events and effectively detect the duration of OSA events [29,30]. By exploiting the sensitivity of delta waves in a sleep cycle, the frequency variation approach transforms the frequency ratio of delta wave in sleep signals into frequency variations. This approach accurately estimates the start and end times of OSA events rather than simply classifies information into different categories. However, the principal drawback of the frequency variation approach is that it can only detect the duration of complete OSA events, not the start and end time points of incomplete events [15]. Additionally, the approach may also misclassify a single OSA event as multiple events, or *vice versa*.

The relationship between the human left and right brain is sustained by biological pathways that deliver messages and maintain close connections between the two hemispheres [2]. The functional asymmetry of the brain has attracted significant interest in recent years, and discoveries made by recent studies have been applied to different diseases such as Alzheimer's disease and epilepsy [2,10,12]. The EEG spectral energy in the transition from non-rapid eye movement (NREM) to rapid eye movement (REM) varies for certain bands [35]. Abeyrantne et al. utilized interhemispheric signals to identify correlations between the interhemispheric synchrony index (IHSI) and RDI [2]. However, the IHSI must be converted according to the whole data of each case, hindering detection of the duration of each OSA event. Moreover, the time resolution for an OSA event is low and detecting its precise time of occurrence is difficult. Therefore, OSA events cannot be identified effectively.

This work uses the brainwaves features of the left and right hemispheres to estimate the duration of incomplete OSA events. By detecting changes in EEG signals from the left and right hemispheres during OSA events, the start and end time of incomplete OSA events can be inferred based on the detected duration of complete OSA events. Experimental results show that the proposed approach substantially improves the accuracy of OSA event detection in terms of the aspects of time and the performance of overall system.

The remainder of this paper is organized as follows. Section 2 reviews related work of feature extraction and interhemispheric analysis of EEG signals. Section 3 introduces the architecture of the proposed system. Section 4 discusses experiment results. Section 5 gives conclusions.

2. **Feature Extraction and Interhemispheric Analysis of EEG Signals.** Existing EEG feature extraction approaches can be classified into statistical and frequency-space approaches [7-9,19,24,26,28,40,41]. Statistical approaches usually combine neural networks with statistical features to determine whether variations among samples are apparent based on deviations in statistical calculations. These approaches analyze the relationships among numerous unknown nonlinear and decision variables through neuronal interactions processed by neural networks [31]. For example, Subasi extracted the wavelet coefficient as features to detect epileptic seizures using dynamic fuzzy neural networks [32]. Subasi further extracted wavelet coefficients by transforming EEG signals through the discrete wavelet [33]. Subasi then applied the extracted wavelet coefficients to calculate statistical features, such as the mean absolute value of coefficients, average power of wavelet coefficients, standard deviation of coefficients, and ratio of absolute mean values of adjacent sub-bands. The acquired values were subsequently used to analyze the correlation between awake and sleep states. Ubeyli, who also used EEG signals to extract discrete wavelet coefficients, employed the wavelet coefficient to calculate statistical features, such as mean absolute value of wavelet coefficient, absolute maximum value of wavelet coefficient, average power, standard deviation, ratio of absolute mean values of adjacent sub-bands, comparisons of distortions in the distribution coefficient [37], and maximum, minimum, mean, and standard deviation to detect epilepsy through multilayer perceptron neural networks (MLPNNs) [38,39]. Kurt used EEG signals to identify stages 0 and 1 in sleep cycles [18]. The signals of EEGs, electrooculograms, and electromyograms were first transformed by a discrete wavelet, filter, and the filtered frequency spectrum. Data obtained were subsequently analyzed using MLPNNs to identify the correlation between awake and sleep states. Guo, who used the frequency variation and amplitude of signals as a line length feature, employed the length of the delta wave line in EEG signals to detect epilepsy, Alzheimer's disease, and Parkinson's disease [10].

The approach using frequency-space relationships quantifies the frequency and space features of various abnormal brainwaves using EEG signal-frequency-related features or time and space features. For example, Ocak et al. detected epilepsy using approximate entropy and discrete wavelet coefficients extracted from EEG signals as features [29]. Hsu extracted the delta, theta, alpha, and beta waves using discrete wavelet transformation, and obtained normalized EEG signal features, such as time lag, embedding dimension, correlation dimension, and the largest Lyapunov exponent, and subsequently detected the duration of an epileptic fit using a support vector machine [14]. Yildiz et al., who calculated the approximate entropy of EEG signals, evaluated changes from the awake to sleeping state using an adaptive neuro fuzzy inference system [41]. Ko et al. extracted EEG signal features using the fast Fourier transform (FFT) and principle component analysis, followed by cross-validation using linear regression, radial basis function neural networks, and support vector regression to estimate the correlation between motion sickness and EEG signals [17]. Aris et al. performed data partitioning and developed a linear regression model using signals from the right and left hemispheres to extract the features of slope and relative average power [5]. Fuzzy C-mean analysis was then applied to categorize brain activity and recognition and management behaviors.

Interhemispheric signals are analyzed by extracting brainwave features using correlation and statistical analysis to determine the interhemispheric connection or synchrony of the cerebral cortex [2,6,35]. Abeyratne et al. extracted delta, theta, alpha, and beta waves and the time series of interhemispheric asynchrony (IHA) by transforming EEG signals in the C3/A1 and C4/A2 regions using the FFT approach [2]. Abeyratne et al. then calculated the mean, standard deviation, variance, skewness, and kurtosis of each wave to distinguish between NREM and REM. Finally, principal components were analyzed and

crucial feature vectors were screened to calculate the IHSI values and RDI correlation. Khandoker et al. calculated the power spectral density of various waves during and after OSA events using an EEG and electrocardiogram (ECG), and identified the correlation between each factor using coherence analysis [16]. To examine differences in airflow and blood oxygen level (SaO2) of OSA patients, Alvarez et al. also utilized coherence analysis [4]. Hsu and Chiu applied analysis of variance to analyze EGG signal features, including the spectral profile, energy ratio, interhemispheric alpha coherence, and intrahemispheric alpha coherence, to determine changes in brainwaves of Alzheimer's patients [13]. Hidasi et al. identified a correlation between Alzheimer's disease and the theta wave by identifying differences between long and short ranges and each region of the left and right hemispheres using relative frequency spectra, the FFT, and synchrony analysis [12]. Sezgin and Tagluk calculated the quadratic phase coupling of each wave in EEG signals of OSA patients using bispectral analysis, and determined the phase coupling phenomenon using the MLPNNs [30].

3. **System Architecture.** Figure 1 shows the architecture of the proposed incomplete OSA event detection system. This system has two modules: a feature extractor, and OSA discriminator. The former extracts frequency variations from EEG brainwaves between the left and right hemispheres, while the latter determines the time-frequency of incomplete OSA events based on brainwaves of the left and right hemispheres. The functionality of each module is discussed as follows.
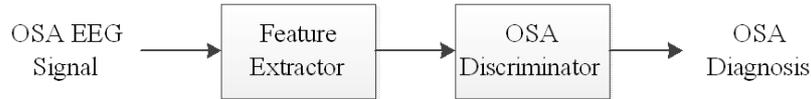
FIGURE 1. System architecture

3.1. **Feature extractor.** The feature extractor calculates frequency variation, slope, and mean variance of brainwave signals in the left and right hemispheres (i.e., C3-A1 and C4-A2) of OSA patients. Frequency variation (V) detects the delta wave frequency variation of delta waves in the left and right hemispheres by calculating the frequency variation of delta waves at the start and end of OSA events.

$$V = \left| \frac{\sum_{i=T_{start}}^{i=T_{end}} (y_{i+1} - y_i)}{T_{end} - T_{start} - 1} \right| \tag{1}$$

where y, T_{start}, and T_{end} are the ratio of the delta wave, start time, and end time of an OSA event, respectively. The start time is the time when the delta wave curve begins declining to the time when this decline stops. End time is the time the next delta wave cycle begins declining. The proportion of the delta wave is determined by extracting 0-32 Hz signals using bandpass filters, followed by removing the ratio of the delta waveform from the alpha, beta, theta, delta, and sigma waves via empirical mode decomposition and the Hilbert-Huang transformation (Figure 2) [15].

Slope (S) is the declining slope value of the delta wave from the start to the end of an OSA event.

$$S = \frac{Y_{T_1} - Y_{T_2}}{X_{T_1} - X_{T_2}} * 100 \tag{2}$$

where (X_{T_1}, Y_{T_1}) represents the start time of OSA within the delta waveform, and (X_{T_2}, Y_{T_2}) represents the time point when waveform decline terminates (Figure 3).
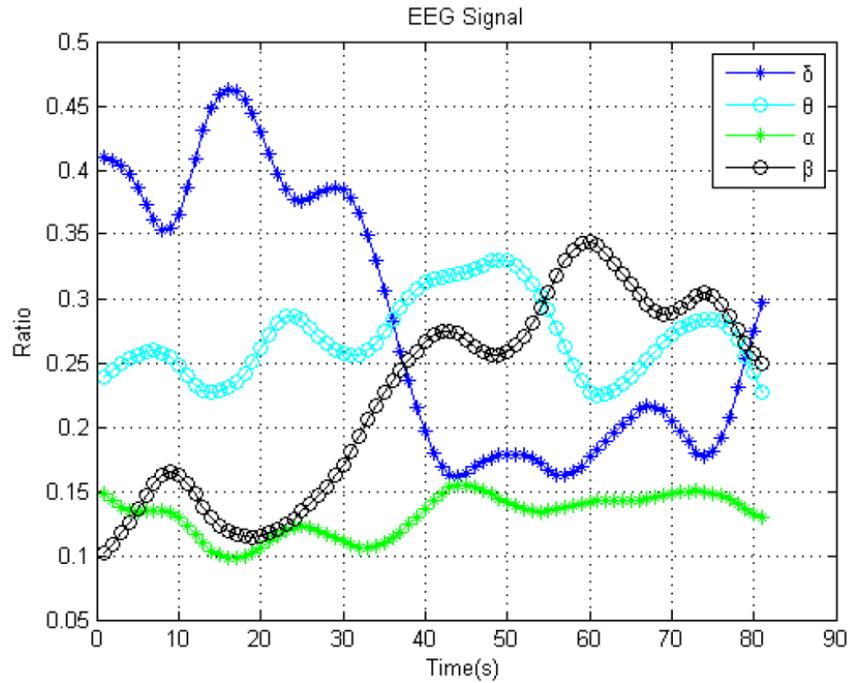
FIGURE 2. The ratio of each band in an EEG
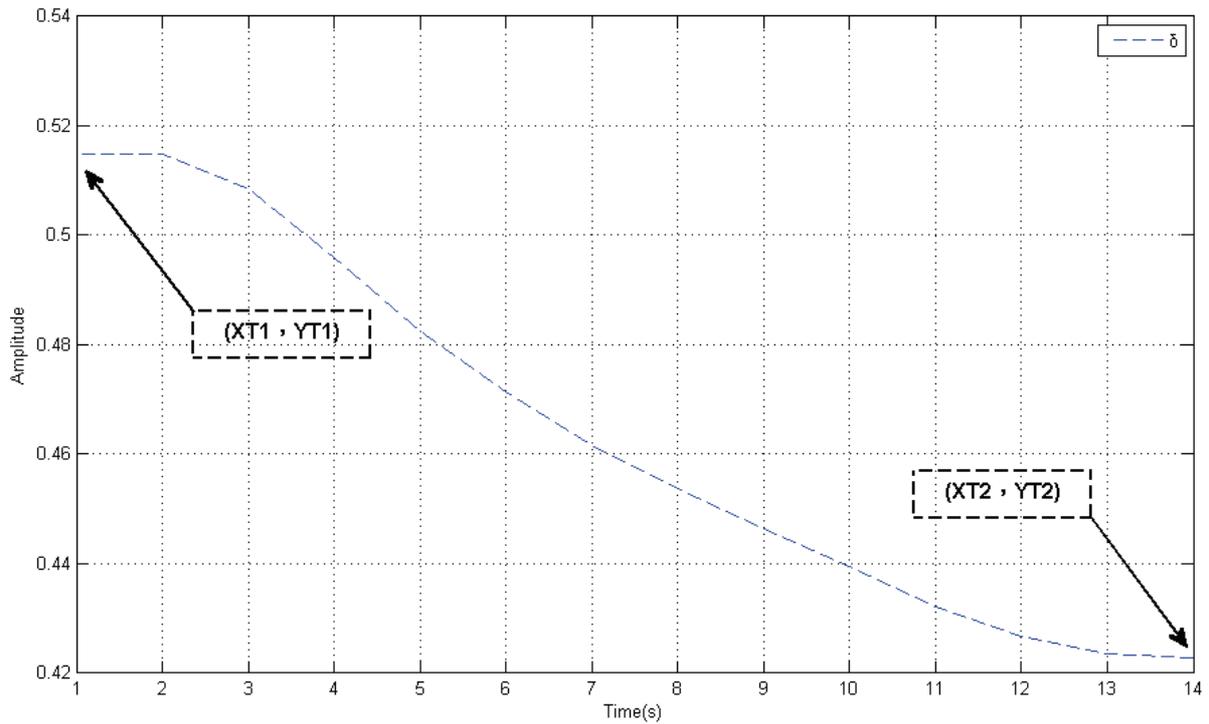
FIGURE 3. Start and end time of an OSA event

The average variation (A) calculates the average variation of the delta waveform in brainwaves from the left and right hemispheres during an OSA event.

$$A = \sum\nolimits_{j=T_{end}}^{j=T_{start}} \sqrt{(Y_j - Y_{j-1})^2 + 1} \qquad (3)$$

where Y_j, T_{start}, and T_{end} are the amplitude of the delta wave at time j, and start and end time of an OSA event, respectively.

3.2. **OSA discriminator.** The OSA discriminator detects the time at which an OSA event occurs and adjusts the time at which an incomplete OSA event happens. The start and end time points of OSA events are detected by monitoring the frequency variation of delta waves.

$$T_{start} = \text{if } V \leq \text{Threshold}_1 \tag{4}$$

$$T_{end} = \text{if } V \geq \text{Threshold}_2 \tag{5}$$

where T_{start}, T_{end} and V are the start time of an OSA event, end time of an OSA event, and frequency variation, respectively. Threshold$_1$ and Threshold$_2$ are used to determine whether frequency variation is above or below the threshold value. The incomplete time adjustment is used to estimate the start or end time of an incomplete OSA event when only the end or start time is detected.

$$T_{start} = T_{end} - T \text{ or } T_{end} = T_{start} + T \tag{6}$$

where T is the average duration of OSA events. The function of average duration is used to determine the relationship between average time and frequency variation in all detected OSA events of a patient.

$$T = CV + K - |S - S'| \times W \tag{7}$$

$$K = \frac{k_1 + k_2}{2} \tag{8}$$

where C, V, W, S, S', k_1, and k_2 are the slope of duration time regarding frequency variation, frequency variation of incomplete OSA events, weight, slope of incomplete OSA events, average slope of the average displacement of known OSA events, maximum displacement during OSA events, and minimum displacement during OSA events, respectively. Notably, T1 and T2 are parallel lines formed by connecting the uppermost and bottommost duration *versus* frequency variation points in all detected OSA events; T is the parallel line formed by connecting the average displacement of the uppermost and bottommost duration time *versus* frequency variation. The optimized weights are
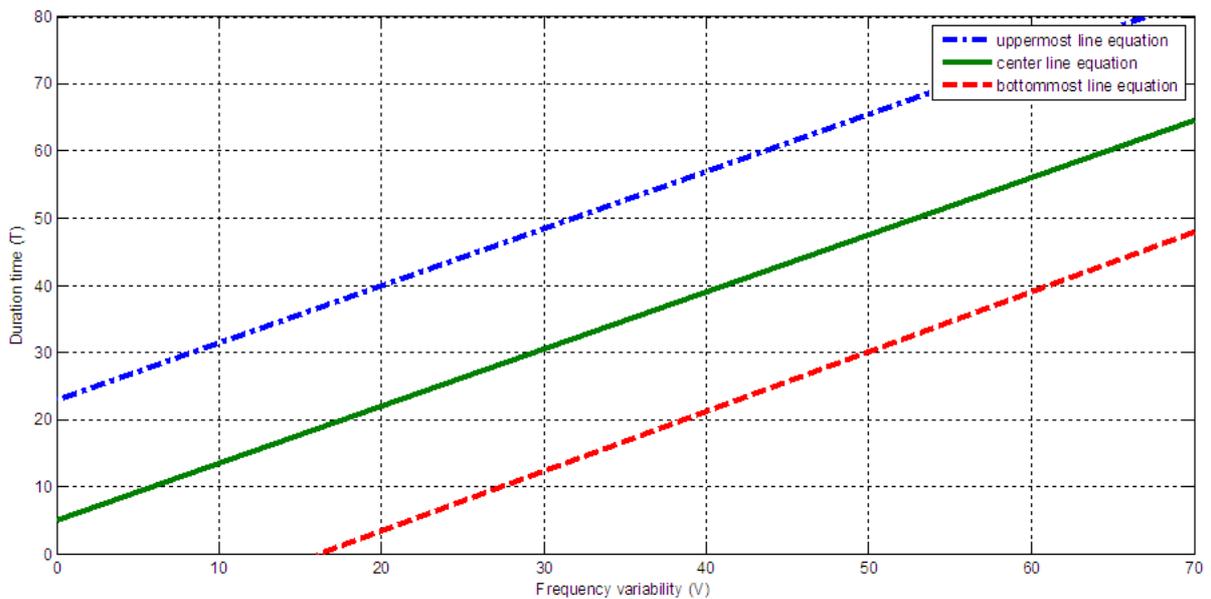
FIGURE 4. Relationship between average time and frequency variation during OSA events

the weights adjusted by a genetic algorithm to find the minimal error between detected duration and a patient's practical duration of all OSA events.

4. **Experimental Results.** Experimental data were obtained from the sleep center at Shin Kong Wu Ho-Su Memorial Hospital, Taipei City, Taiwan. The brainwave data of the left and right hemispheres (i.e., C3-A1 and C4-A2) were collected from all-night sleep records of OSA patients. All patients had severe OSA, and were aged 31-72 (Table 1).

4.1. **Feature extractor.** Figures 5 and 6 show original EEG signals of the left and right hemispheres of case 11, respectively. Figures 7 and 8 show the EEG signals and their delta wave ratios between the left and right hemispheres processed by feature extractors, respectively.

   Table 2 lists the OSA events of case 11. Figures 9 and 10 show the delta wave ratios and waveforms of case 11, respectively. The start time point of an OSA event is 9358 s,

TABLE 1. Example cases

	Age	Sex	OSA	RDI
Case 1	58	Male	38	36.3
Case 2	40	Female	122	75.8
Case 3	72	Male	24	47.8
Case 4	48	Male	66	47.2
Case 5	51	Female	27	30.4
Case 6	58	Male	11	45.4
Case 7	60	Male	18	63.2
Case 8	31	Male	142	61.8
Case 9	66	Male	27	36.2
Case 10	45	Male	68	63.9
Case 11	49	Male	11	63.9
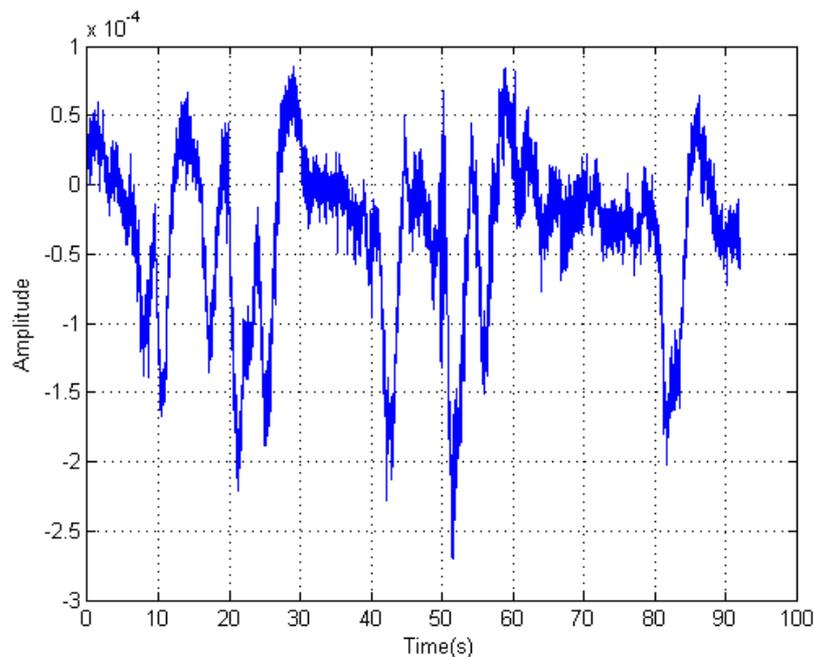
FIGURE 5. Example of the original EEG signal of the left hemisphere
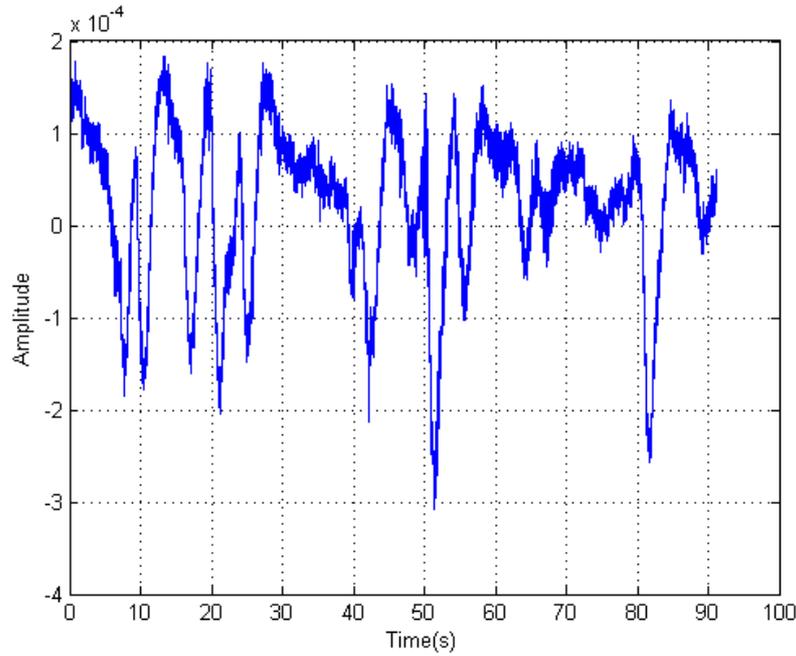
FIGURE 6. Example of the original EEG signal of the right hemisphere
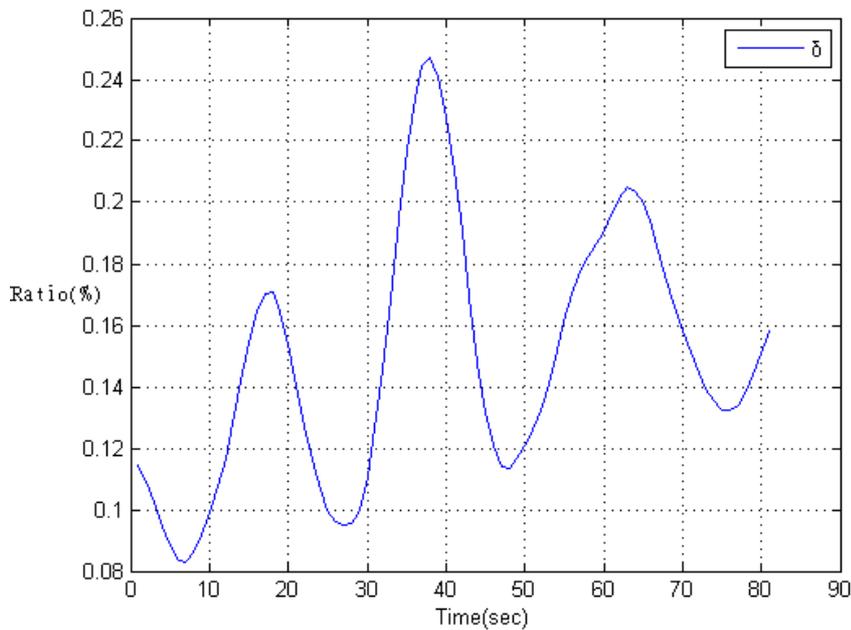
FIGURE 7. Delta wave ratio of the left hemisphere

and the end point is 9379 s. The maximum amplitude of delta wave frequency variability is 0.23, and minimum amplitude is 0.14. The calculated frequency variation, slope, and average variation of case 11 are 0.0045, -0.4267, and 0.0041, respectively. Figure 11 displays the start time of the delta wave $(9358, 0.23)$ and the time when the waveform stops declining $(9379, 0.14)$ during OSA events.

4.2. **OSA discriminator.** The main task of the OSA discriminator is to identify the time duration of OSA events; Threshold_1 and Threshold_2 are defined as 0.01 and -0.01,
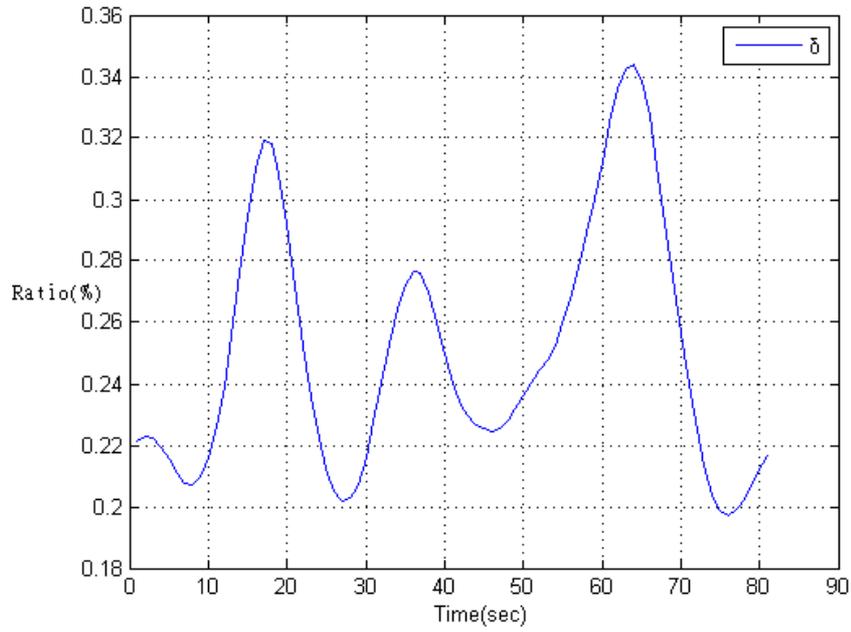
FIGURE 8. Delta wave ratio of the right hemisphere

TABLE 2. Data points of the OSA event in Figure 9

Time (s)	Value
9358	0.23
9359	0.23
9360	0.23
9361	0.23
9362	0.22
9363	0.22
9364	0.22
9365	0.22
9366	0.22
9367	0.22
9368	0.21
9369	0.21
9370	0.20
9371	0.19
9372	0.18
9373	0.17
9374	0.17
9375	0.16
9376	0.15
9377	0.14
9378	0.14
9379	0.14
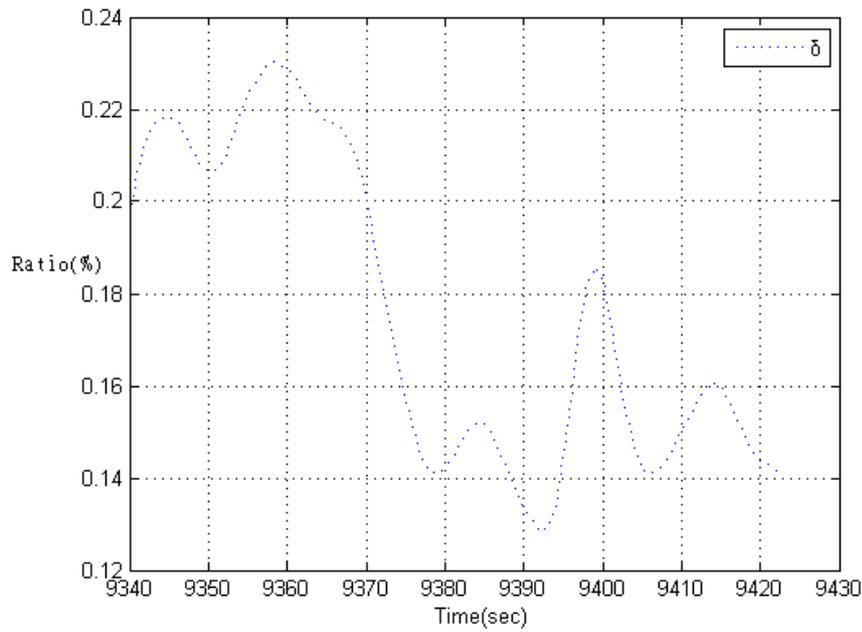
FIGURE 9. An OSA event in the right hemisphere of case 11
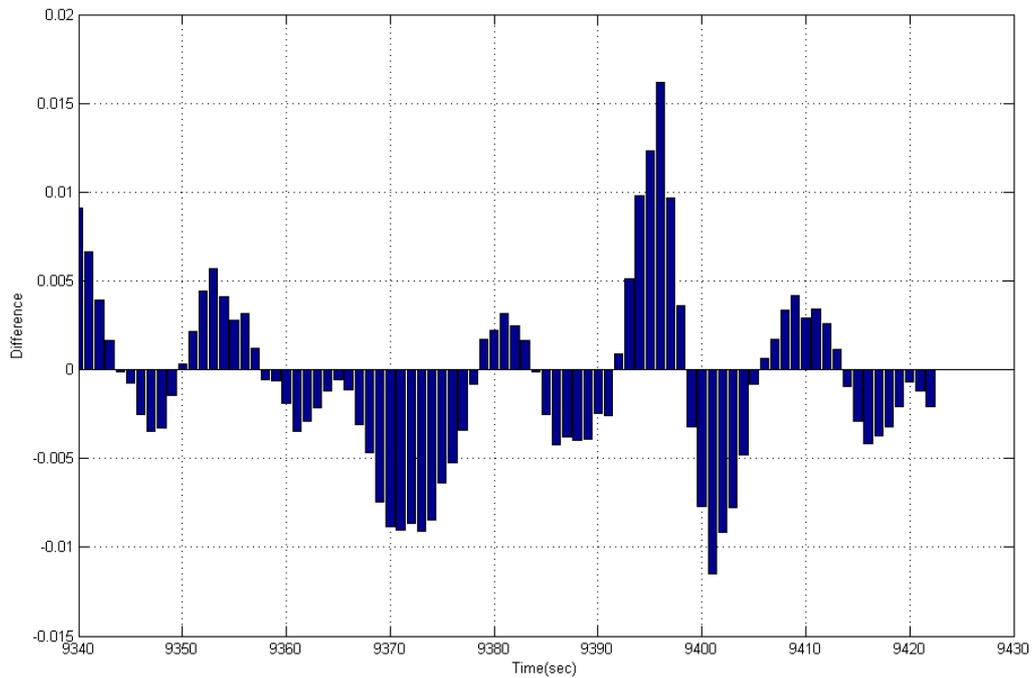
FIGURE 10. Frequency variation of the delta wave

respectively. The duration and frequency variation of complete OSA events in brainwaves of the left and right hemispheres of all cases are marked (Figures 12 and 13). The slope of time versus frequency variation is 0.86. The maximum displacement of k_1 is 22.48 and minimum displacement of k_2 is -12.52. Thus, duration displacement is 4.98 during the OSA event.
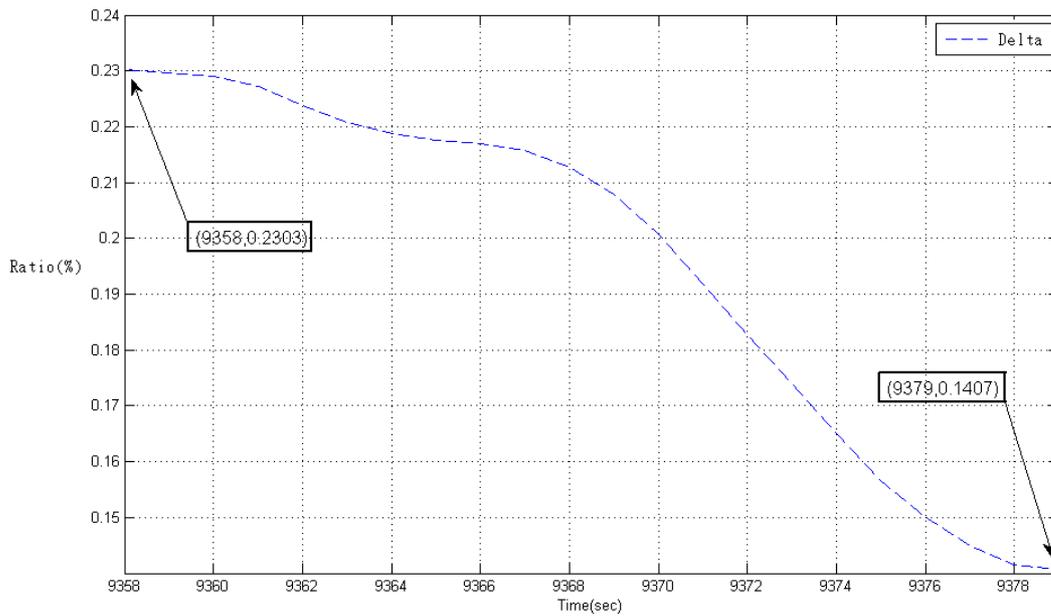
FIGURE 11. Start and end time of an OSA event in the delta wave
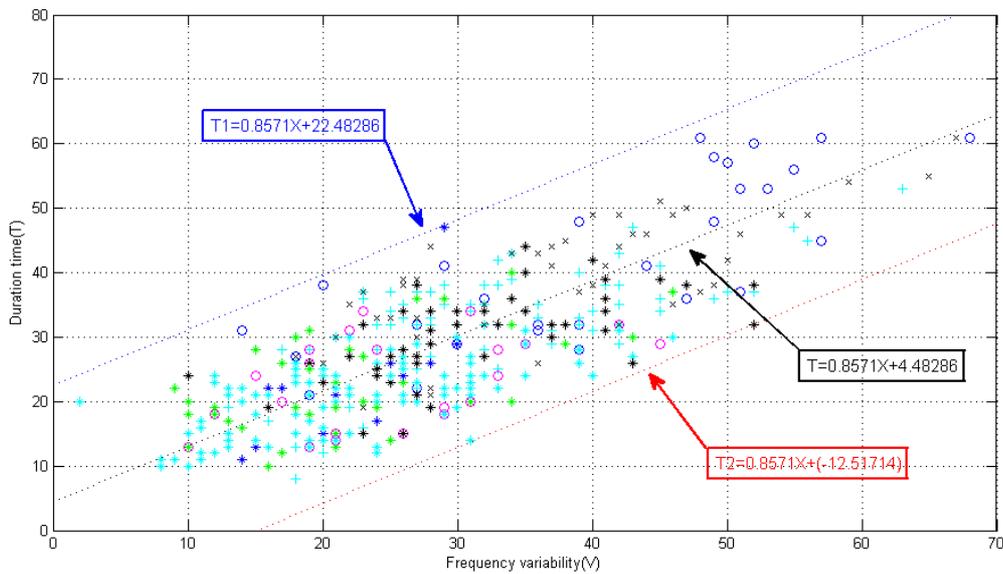
FIGURE 12. Average time *versus* frequency variation of OSA events in the left hemisphere

Figure 14 shows the left and right hemisphere signals of case 11. For the left hemisphere signal, the slope of incomplete OSA events is -1.35; average slope displacement of a known OSA event is -1.01; and average duration of a complete OSA event is 46 s. The value of W, T, and T_{end} are 26, 6.48, and 3260, respectively. For the right hemisphere signal, the slope of the incomplete OSA event is -0.43; average slope displacement of an OSA event is known to be -1.01; and the average duration of a complete OSA event is 13 s.

Table 3 shows the number of complete and incomplete OSA events in the left hemisphere. Tables 4, 5, and 6 show the detected frequency of a complete OSA event in the
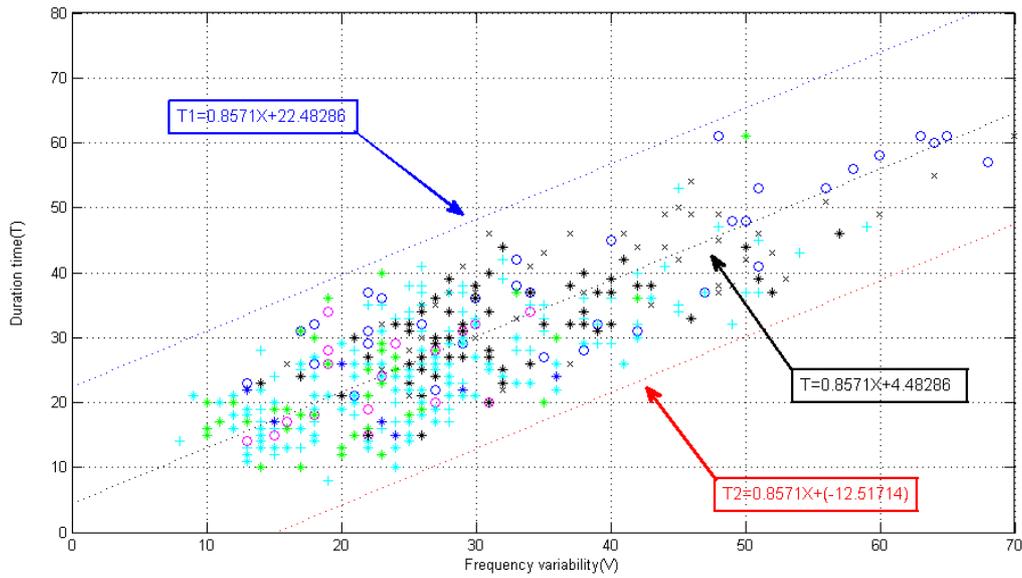
FIGURE 13. Average time *versus* frequency variation of OSA events in the right hemisphere
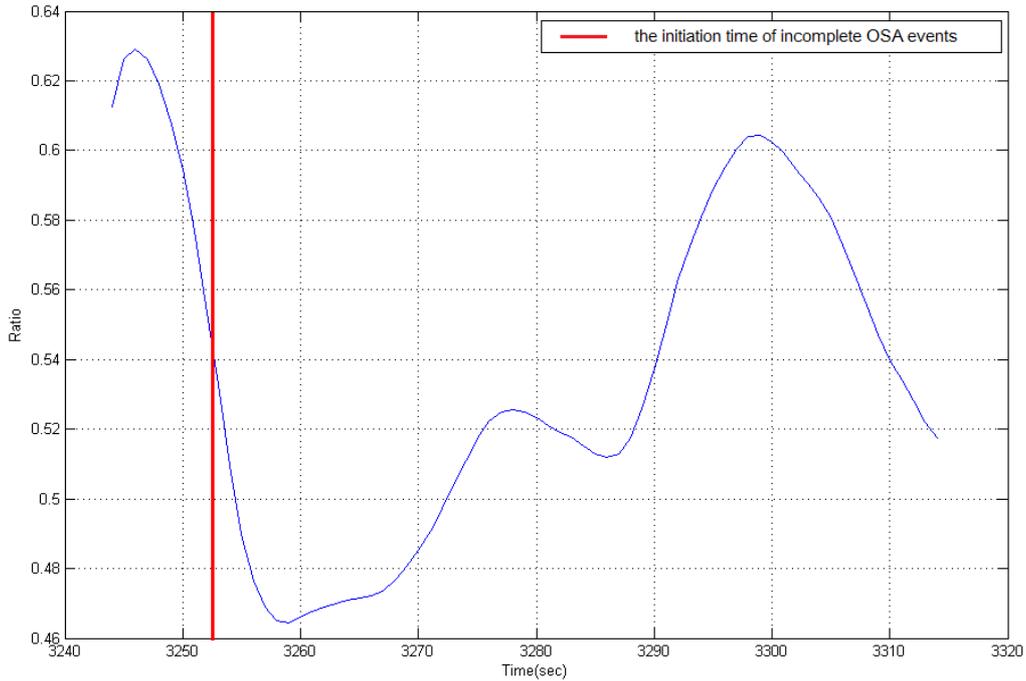
FIGURE 14. Start time of an incomplete OSA event

left hemisphere, average error of the start and end time of detected OSA events, and experimental results for duration of incomplete OSA events in the left hemisphere. Table 7 shows the number of complete OSA events and incomplete OSA events in the right hemisphere. Tables 8, 9, and 10 show experimental results for the time-frequency of complete OSA events, average error of the start and end time of detected OSA events in the

right hemisphere, and experimental results for the number of incomplete OSA events in the right hemisphere.

Comparisons of signals from the left and right hemispheres for feature extraction and OSA discrimination indicate that estimations of the start and end time of detected OSA events based on the left hemisphere were more accurate than those based on the right hemisphere. The accuracy for the number of OSA events for the left and right hemispheres is 95.45% and 93.45%, respectively. The accuracy for the duration of OSA events for the left and right hemispheres is 88% and 83%, respectively. Therefore, the left hemisphere is the more helpful brainwave signal feature for detecting OSA events.

4.3. **Comparisons.** This work uses patient data to compare variations among similar approaches, namely, approaches used by the frequency variation method, and by Abeyratne et al., and Guo [2,10]. The frequency variation method uses the Hilbert-Huang transform to determine the ratio of each band in brainwaves, and monitors the trend of frequency variation of the delta wave to detect the time an OSA event occurs. Figure 15 and Tables 11 and 12 show the detected power spectral density and accuracy. Abeyratne used the

TABLE 3. Number of complete and incomplete OSA events in the left hemisphere

	# of complete OSA event	# of incomplete OSA event
Case 1	33	5
Case 2	89	33
Case 3	17	7
Case 4	53	13
Case 5	22	5
Case 6	10	1
Case 7	15	3
Case 8	109	33
Case 9	19	8
Case 10	41	27
Case 11	8	3

TABLE 4. Experimental result for complete OSA events in the left hemisphere

	# of OSA event	# of detected OSA event	# of the same OSA duration	# Accuracy of detected OSA event
Case 1	38	36	33	94.73%
Case 2	122	120	89	97.36%
Case 3	24	23	17	98%
Case 4	66	65	53	98.48%
Case 5	27	26	22	98%
Case 6	11	10	10	99%
Case 7	18	17	15	98%
Case 8	142	138	109	97.88%
Case 9	27	25	19	92.59%
Case 10	68	64	41	94.11%
Case 11	11	8	8	81.81%

TABLE 5. Average error of start and end time in the left hemisphere

	Average error of start time	Average error of end time
Case 1	5.82	5.5
Case 2	4.97	4.33
Case 3	5.55	4.95
Case 4	5.12	4.05
Case 5	5.74	3.42
Case 6	5.95	6.09
Case 7	6.13	6.65
Case 8	5.06	4.18
Case 9	3.9	5.95
Case 10	4.49	8.17
Case 11	4.83	7.88

TABLE 6. Experimental result for incomplete OSA events in the left hemisphere

	# of incomplete OSA event	Weight	Time accuracy
Case 1	5	36	80%
Case 2	33	22	82%
Case 3	7	0.25	84.88%
Case 4	13	38	86.26%
Case 5	5	21	94.90%
Case 6	1	0.25	90.46%
Case 7	3	14	86.82%
Case 8	33	25	90.51%
Case 9	8	16	80.98%
Case 10	27	26	92.83%
Case 11	3	0.25	90%

TABLE 7. Number of complete and incomplete OSA events in the right hemisphere

	# of complete OSA event	# of incomplete OSA event
Case 1	33	5
Case 2	91	31
Case 3	19	5
Case 4	51	15
Case 5	18	9
Case 6	8	3
Case 7	13	5
Case 8	103	39
Case 9	27	0
Case 10	58	10
Case 11	3	8

TABLE 8. Experimental result of complete OSA events in the right hemisphere

	# of OSA event	# of detected OSA event	# of the same OSA duration	# Accuracy of detected OSA event
Case 1	38	37	33	98%
Case 2	122	121	91	98.18%
Case 3	24	23	19	93.83%
Case 4	66	64	51	96.97%
Case 5	27	25	18	96.92%
Case 6	11	10	8	94%
Case 7	18	17	13	95%
Case 8	142	139	103	97.59%
Case 9	27	25	27	94.37%
Case 10	68	64	58	94.11%
Case 11	11	10	3	90.9%

TABLE 9. Average error of start and end time in the right hemisphere

	Average error of start time	Average error of end time
Case 1	5.75	4.66
Case 2	5	4.26
Case 3	5.45	4.84
Case 4	5.32	3.54
Case 5	3.7	5.65
Case 6	6.55	3.56
Case 7	6.77	4.81
Case 8	4.88	4.13
Case 9	4.41	6
Case 10	4.31	6.96
Case 11	8	5.8

FFT approach and calculated the synchronized time series of the left and right hemispheres. Abeyratne then calculated various waves and used principal component analysis to screen crucial components for the feature vector. He also calculated the IHSI value to identify the severity of the corresponding RDI. Finally, IHSI was used as an indicator to identify the OSA event. Events lower than the threshold of 700 were considered OSA events (Figure 16). Guo used wavelet transformation to extract brainwave signal features. The length of the line was regarded as a feature criterion. Next, an MLPNN was used to detect OSA events, 50% of which was used for MLPNN training and 50% was used for MLPNN tests (Figure 17). The approaches used by Guo, Hsu & Shih, and Abeyratne were applied in this study to conduct similar experiments. The experimental results show that though the approaches used by frequency variation method, Guo, and Abeyratne were unable to determine the time at which an OSA event occurred, the proposed approach achieved relatively high accuracy (Table 13).

Table 14 shows previous EEG-based OSA detection systems and compares these systems with the proposed system. Abeyratne used the interhemispheric signals of C3/A1 and C4/A2 to classify the patients into OSA and non-OSA classes. However, the IHSI cannot detect the duration of each OSA event. Tagluk and Sezgin used the C3/A2 signal to
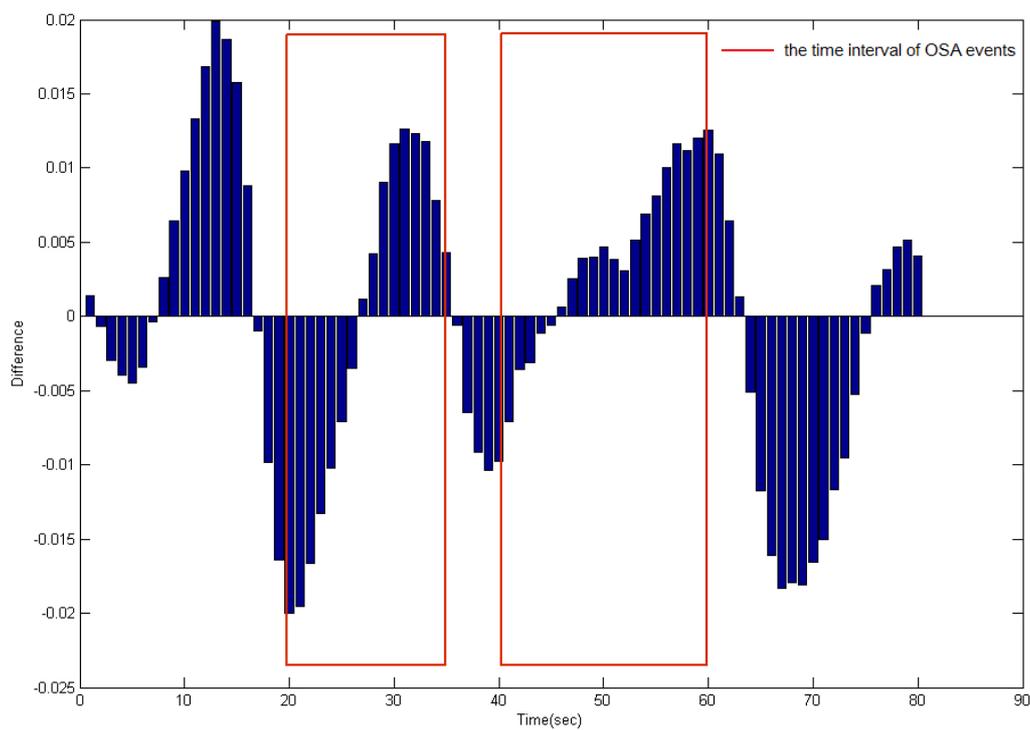
FIGURE 15. Detected power spectral density of delta waves
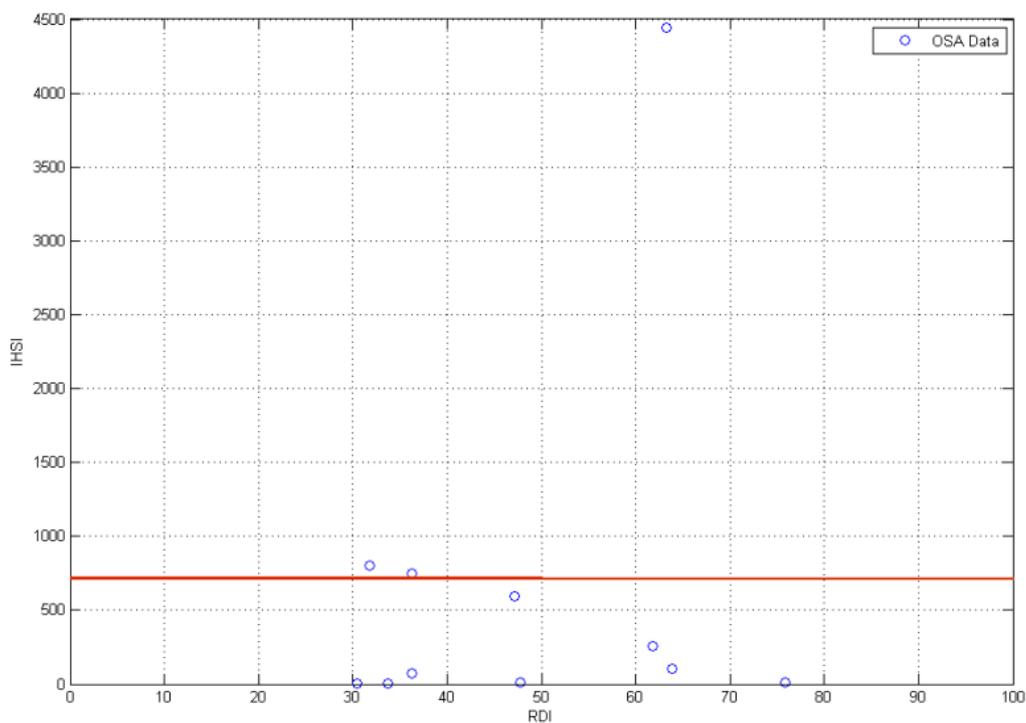
FIGURE 16. IHSI comparison

TABLE 10. Experimental result of incomplete OSA events in the right hemisphere

	# of incomplete OSA event	Weight	Accuracy of detected OSA duration
Case 1	5	35	93.98%
Case 2	31	25	81%
Case 3	5	22	80.97%
Case 4	15	22	83.06%
Case 5	9	25	83.38%
Case 6	3	0.25	93.09%
Case 7	5	0.25	83.25%
Case 8	39	21	84.56%
Case 9	0	0	74.77%
Case 10	10	21	97.30%
Case 11	8	0.25	47.19%

TABLE 11. Experimental results for the left hemisphere

	# of OSA event	# of detected OSA event	Accuracy of detected OSA event	Maximal Accuracy of detected OSA event
Case1	38	33	88.73%	94.73%
Case2	122	110	90.36%	97.36%
Case3	24	20	85%	98%
Case4	66	60.	91.48%	98.48%
Case5	27	24	92%	98%
Case6	11	9.	90.45%	99%
Case7	18	16	89.54%	98%
Case8	142	130	91.55%	97.88%
Case9	27	22	81.48%	92.59%
Case10	68	60	88.23%	94.11%
Case11	11	9	81.81%	81.81%

TABLE 12. Experimental results for the right hemisphere

	# of OSA event	# of detected OSA event	Accuracy of detected OSA event	Maximal Accuracy of detected OSA event
Case 1	38	35	91%	98%
Case 2	122	108	88.18%	97.18%
Case 3	24	22	90.83%	93.83%
Case 4	66	59	89.39%	96.97%
Case 5	27	25	91.92%	94.92%
Case 6	11	10	92.54%	94.00%
Case 7	18	15	83%	95.00%
Case 8	142	127	89.59%	96.59%
Case 9	27	24	90%	92.37%
Case 10	68	60	88.23%	93.11%
Case 11	11	10	88.9%	89.49%
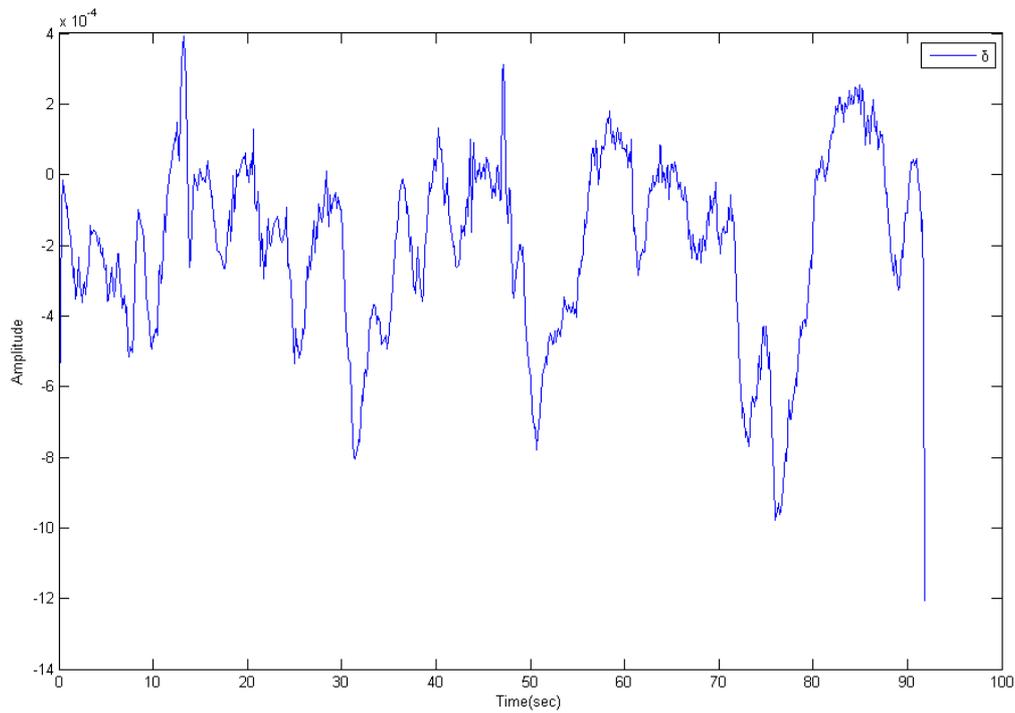
FIGURE 17. Wavelet transformation of delta waves

TABLE 13. Comparison of OSA detection methods

Researchers	Left hemisphere	Right hemisphere
Proposed method	95.78%	92.32%
Hsu & Shih	89.18%	87.09%
Abeyratne	72%	
Guo	78%	74.23%

classify the OSA and non-OSA patients by bispectral analysis and backpropagation neural network [36]. Although Tagluk extracts the signals of alpha, beta, delta, theta, and gamma from OSA events as the features to train the neural network, it cannot detect the duration of each OSA event from all-night brain signals. Hsu & Shih used the frequency variation approach to detect the duration of each OSA event. The system can only detect the duration of complete OSA events. However, it cannot handle incomplete OSA events.

5. **Conclusions.** This work proposes a system for determining the duration of incomplete OSA events using brainwave frequency in the interhemispheric region. The proposed system has two modules: the feature extractor, and OSA discriminator. Delta waves in the left and right hemispheres (i.e., C3-A1 and C4-A2) are extracted by a bandpass filter, and the signal features, such as frequency variation, slope, and average frequency variation, are then calculated. The OSA discriminator uses the relationship between average time and frequency variation of OSA events to search for durations of OSA events, and determines the correct start or end time via effective feature extraction methods to obtain the durations of complete OSA events.

The proposed system has the following advantages over existing approaches. First, the proposed feature discrimination method for assessing OSA events is better than previous

TABLE 14. OSA related systems comparison

	Proposed system	Abeyratne	Tagluk	Hsu & Shih
Brain channel	C3/A1, C4/A2	C3/A1, C4/A2	C3/A2	C3/A2
Brain signals	Delta	Alpha, beta, delta, theta,	Alpha, beta, delta, theta, gamma	Delta
Detection method	Signal features	IHSI	Bispectral analysis, Neural network	Signal features
OSA diagnosis	Event duration	Event occurrence	Event occurrence	Event duration

methods that analyzed features statistically. For extracting crucial brainwave features, this work uses the signal waveform of the delta wave to search for the duration of OSA events. Apparent OSA events are subsequently identified by analyzing brainwave features of OSA events, such as frequency variation, slope, and average frequency variation. The ability to identify OSA events specifically and ability to determine the duration of OSA events allow the system to detect the complete duration and adjust the duration of an incomplete OSA event. To detect incomplete OSA events, the correct start or end time is determined to identify the complete duration of an OSA event, and to establish an accurate and comprehensive detection system. The proposed system can be applied for medical diagnoses to improve the accuracy of OSA event identification.

REFERENCES

[1] H. Abdullah, N. C. Maddage, I. Cosic and D. Cvetkovic, Cross-correlation of EEG frequency bands and heart rate variability for sleep apnoea classification, *Medical & Biological Engineering & Computing*, vol.48, no.12, pp.1261-1269, 2010.

[2] U. R. Abeyratne, V. Swarnkar, C. Hukins and B. Duce, Interhemispheric asynchrony correlates with severity of respiratory disturbance index in patients with sleep apnea, *IEEE Transactions on Biomedical Engineering*, vol.57, no.12, pp.2947-2955, 2010.

[3] N. Acir, Automatic recognition of sleep spindles in EEG by using artificial neural networks, *Expert Systems with Applications*, vol.27, no.3, pp.451-458, 2004.

[4] D. Alvarez, G. C. Gutierrez, J. V. Marcos, F. del Campo and R. Hornero, Spectral analysis of single-channel airflow and oxygen saturation recordings in obstructive sleep apnea detection, *Proc. of the IEEE Conference on Engineering in Medicine and Biology Society*, pp.847-850, 2010.

[5] S. A. M. Aris, M. N. Taib, S. Lias and N. Sulaiman, Feature extraction of EEG signals and classification using FCM, *Proc. of the International Conference on Modelling and Simulation*, pp.54-58, 2011.

[6] C. Babiloni, G. Albertini, P. Onorati, F. Vecchio and P. Buffo, Inter-hemispheric functional coupling of eyes-closed resting EEG rhythms in adolescents with down syndrome, *Clinical Neurophysiology*, vol.120, no.9, pp.1619-1627, 2009.

[7] S. Chandake, A. Chatterjee and S. Munshi, Cross-correlation aided support vector machine classifier for classification of EEG signals, *Expert Systems with Applications*, vol.36, no.2, pp.1329-1336, 2009.

[8] J. Greneche, M. Saremi, C. Erhardt, A. Hoeft, A. Eschenlauer, A. Muzet and P. Tassi, Severity of obstructive sleep apnoea/hypopnoea syndrome and subsequent waking EEG spectral power, *European Respiratory Journal*, vol.32, no.3, pp.705-709, 2008.

[9] S. Gunes, K. polat and S. Yosunkaya, Efficient sleep stage recognition system based on EEG signal using *k*-means clustering based feature weighting, *Expert Systems with Applications*, vol.37, no.12, pp.7922-7928, 2010.

[10] L. Guo, Automatic epileptic seizure detection in EEGs based on line length feature and artificial neural networks, *Journal of Neuroscience Methods*, vol.191, pp.101-109, 2010.

[11] H. G. Jo, J. Y. Park, C. K. Lee, S. K. An and S. K. Yoo, Genetic fuzzy classifier for sleep stage identification, *Computers in Biology and Medicine*, vol.40, no.7, pp.629-634, 2010.

[12] Z. Hidasi, B. Czigler, P. Salacz, E. Csibri and M. Molnár, Changes of EEG spectra and coherence following performance in a cognitive task in Alzheimer's disease, *International Journal of Psychophysiology*, vol.65, no.3, pp.252-260, 2007.

[13] C. Y. Hsu and H. W. Chiu, Clinical EEG-based assessment model for alzheimer's disease, *Journal of Taiwan Association for Medical Informatics*, vol.16, no.2, pp.43-52, 2007.

[14] K. C. Hsu, Detection of seizures in EEG using subband nonlinear parameters and genetic algorithm, *Computers in Biology and Medicine*, vol.40, no.10, pp.823-830, 2010.

[15] C. C. Hsu and P. T. Shih, A novel sleep apnea detection system in electroencephalogram using frequency variation, *Expert Systems with Applications*, vol.38, no.5, pp.6014-6024, 2011.

[16] A. H. Khandoker, C. K. Karmakar and M. Palaniswami, Analysis of coherence between sleep EEG and ECG signals during and after obstructive sleep apnea events, *Proc. of the IEEE Conference on Engineering in Medicine and Biology Society*, pp.3876-3879, 2008.

[17] L. W. Ko, C. S. Wei, T. P. Jung and C. T. Lin, Estimating the level of motion sickness based on EEG spectra, *Proc. of the International Conference on Human-Computer Interaction*, pp.169-176, 2011.

[18] M. B. Kurt, The ANN-based computing of drowsy level, *Expert Systems with Applications*, vol.36, no.2, pp.2534-2542, 2009.

[19] C.-J. Lin, C. Chen and C. Lee, Classification and medical diagnosis using wavelet-based fuzzy neural networks, *International Journal of Innovative Computing, Information and Control*, vol.4, no.3, pp.735-748, 2008.

[20] T. Locatelli, M. Cursi, D. Liberati, M. Franceschi and G. Comi, EEG coherence in Alzheimer's disease, *Electroencephalography and Clinical Neurophysiology*, vol.106, no.3, pp.229-237, 1998.

[21] A. Mathieu, S. Mazza, D. Petit, A. Decary, J. M. Marquez, J. Malo and J. Montplaisir, Does age worsen EEG slowing and attention deficits in obstructive sleep apnea syndrome? *Clinical Neurophysiology*, vol.118, no.7, pp.1538-1544, 2007.

[22] A. A. Morsy and K. M. A. Ashmouny, Sleep apnea detection using an adaptive fuzzy logic based screening system, *Proc. of the IEEE Conference on Engineering in Medicine and Biology Society*, vol.6, pp.6124-6127, 2005.

[23] A. F. Q. Manrique, J. B. A. Hernández, C. M. T. González, M. A. F. Ballester and G. C. Domínguez, Detection of obstructive sleep apnea in ECG recordings using time-frequency distributions and dynamic features, *Proc. of the IEEE Conference on Engineering in Medicine and Biology Society*, pp.5559-5562, 2009.

[24] J. V. Marcos, R. Hornero, D. Alvarez, F. D. Campo and C. Zamarron, Assessment of four statistical pattern recognition techniques to assist in obstructive sleep apnoea diagnosis from nocturnal oximetry, *Medical Engineering & Physics*, vol.31, no.8, pp.971-978, 2009.

[25] N. Mohamed, D. Rubin and T. Marwala, Detection of epileptiform activity in human EEG signals using Bayesian neural networks, *Neural Information Processing – Letters and Reviews*, vol.10, no.1, pp.1-10, 2006.

[26] S. P. Nair, D. S. Shiau, J. C. Principe, L. D. Iasemidis, P. M. Pardalos, W. M. Norman, P. R. Carney, K. M. Kelly and J. C. Sackellares, An investigation of EEG dynamics in an animal model of temporal lobe epilepsy using the maximum Lyapunov exponent, *Experimental Neurology*, vol.216, no.1, pp.115-121, 2009.

[27] T. Ning and J. D. Bronzino, Bispectral analysis of the rat EEG during various vigilance states, *IEEE Transactions on Biomedical Engineering*, vol.36, no.4, pp.497-499, 1989.

[28] Y. Nishihara, J. Irie, T. Yamaguchi, T. Yamazaki and K. Inoue, The statistical estimation method of muscle activity based on surface EEG, *ICIC Express Letters, Part B: Applications*, vol.2, no.3, pp.603-607, 2011.

[29] H. Ocak, Automatic detection of epileptic seizures in EEG using discrete wavelet transform and approximate entropy, *Expert Systems with Applications*, vol.36, no.2, pp.2027-2036, 2009.

[30] N. Sezgin and M. E. Tagluk, A new approach for estimation of obstructive sleep apnea syndrome, *Expert Systems with Applications*, vol.38, no.5, pp.5346-5351, 2011.

[31] M. M. Shaker, EEG wave classifier using wavelet transform and fourier transform, *International Journal of Biological and Life Sciences*, vol.1, no.2, pp.85-90, 2005.

[32] A. Subasi, Automatic recognition of alertness level from EEG by using neural network and wavelet coefficients, *Expert Systems with Applications*, vol.28, no.4, pp.701-711, 2005.

[33] A. Subasi, Automatic detection of epileptic seizure using dynamic fuzzy neural networks, *Expert Systems with Applications*, vol.31, no.2, pp.320-328, 2006.

[34] D. P. Subha, P. K. Joseph, R. Acharya U and C. M. Lim, EEG signal analysis: A survey, *Journal of Medical Systems*, vol.34, no.2, pp.195-212, 2010.

[35] V. Swarnkar, U. R. Abeyratne and C. Hukins, Inter-hemispheric asynchrony of the brain during events of apnoea and EEG arousals, *Physiological Measurement*, vol.28, no.8, pp.869-880, 2007.

[36] M. E. Tagluka and N. Sezgin, A new approach for estimation of obstructivesleepapnea syndrome, *Expert Systems with Applications*, vol.38, no.5, pp.5346-5351, 2011.

[37] E. D. Ubeyli, Combined neural network model employing wavelet coefficients for EEG signal classification, *Digital Signal Processing*, vol.19, no.2, pp.297-308, 2009.

[38] E. D. Ubeyli, Lyapunov exponent/probabilistic neural networks for analysis of EEG signals, *Expert Systems with Applications*, vol.37, no.2, pp.985-992, 2010.

[39] E. D. Ubeyli, Least squares support vector machine employing model-based methods coefficients for analysis of EEG signals, *Expert Systems with Applications*, vol.34, no.1, pp.223-239, 2010.

[40] T. Yamaguchi, K. Nagata, P. Q. Truong, M. Fujio and K. Inoue, Pattern recognition of EEG signal during motor imagery by using SOM, *International Journal of Innovative Computing, Information and Control*, vol.4, no.10, pp.2617-2730, 2008.

[41] A. Yildiz, M. Akin, M. Poyraz and G. Kirbas, Application of adaptive neuro-fuzzy inference system for vigilance level estimation by using wavelet-entropy feature extraction, *Expert Systems with Applications*, vol.36, no.4, pp.7390-7399, 2009.